Orographic Constraints on a Modeled Siberian Snow–Tropospheric–Stratospheric Teleconnection Pathway

GAVIN GONG AND DARA ENTEKHABI

Department of Civil and Environmental Engineering, Massachusetts Institute of Technology, Cambridge, Massachusetts

JUDAH COHEN

Atmospheric and Environmental Research, Inc., Lexington, Massachusetts

(Manuscript received 7 April 2003, in final form 1 August 2003)

ABSTRACT

Previous modeling studies have identified a teleconnection pathway linking observation-based early season Siberian snow perturbations to a modulation of the winter Arctic Oscillation (AO) mode. In this study, the key role of orography in producing this modeled teleconnection is explicitly investigated using numerical experiments analogous to the previous studies. The climatic response to the same snow perturbation is investigated under modified orographic barriers in southern and eastern Siberia. Reducing these barriers results in a weakening of the prevailing orographically forced region of stationary wave activity centered over Siberia, as well as the snow-forced upward wave flux anomaly that initiates the teleconnection. This diminished anomaly propagates upward, but does not extend into the stratosphere to weaken the polar vortex. Consequently, poleward refraction of upper-tropospheric waves and downward propagation of coupled wave–mean flow anomalies, which ultimately produce the negative winter AO response, fail to develop. Thus, the mountains represent an orographic constraint on the snow–AO teleconnection pathway. By reducing the orographic barrier, the snow-forced influx of wave energy remains in the troposphere and, instead, produces a hemispheric-scale equatorward wave refraction.

1. Introduction

The dominant mode of Northern Hemisphere atmospheric variability is generally referred to in the literature using the terms North Atlantic Oscillation (NAO; Hurrell 1995), Arctic Oscillation (AO; Thompson and Wallace 1998), and Northern Annular Mode (NAM; Thompson and Wallace 2001). This pattern of climate variability (hereafter referred to as the AO) is now recognized as a fundamental and internal mode of the atmosphere, especially during the winter (Baldwin 2001; Feldstein 2002; Gong et al. 2002). Nevertheless, numerous studies have demonstrated the ability of external forcings to at least modulate, if not initiate, the AO mode of variability (e.g., Cohen and Entekhabi 1999; Baldwin and Dunkerton 1999; Rodwell et al. 1999; Christiansen 2000; Robertson 2001). One such external modulator, land surface snow, is the subject of this study.

Recent literature suggests that interannual land surface snow anomalies can influence interannual variability of the winter AO mode. Observational analyses attribute the decadal-scale negative to positive AO climate shift that occurred in winter 1989 to the anomalously low Eurasian snow cover of the preceeding autumn (Watanabe and Nitta 1999). Significant interannual correlations over 28 yr have been reported between observed Eurasian snow cover and various winter AO indices (Cohen and Entekhabi 1999, 2001; Cohen et al. 2001; Saito et al. 2001). Similarly, exploratory, generally small-ensemble, GCM studies using idealized snow perturbations have suggested a causal relationship between snow and winter climate (Walland and Simmonds 1997; Watanabe and Nitta 1998; Gong et al. 2002). The literature relating snow and Northern Hemisphere climate has been summarized by the authors in Gong et al. (2003a; hereafter GEC03).

Most recently, GEC03 utilized large-ensemble (20) GCM integrations to demonstrate a clear winter AO mode modulation in response to realistic, observation-based Siberian snow perturbations. Furthermore, they identified a physically based teleconnection pathway involving wave–mean flow interaction processes throughout the troposphere and stratosphere, consistent with both established theory and recent literature. A positive Siberian snow perturbation was found to increase local upward stationary wave activity, via diabatic heating anomalies commonly associated with snow anomalies (Cohen 1994). The wave activity anomalies propagate

Corresponding author address: Gavin Gong, Department of Earth and Environmental Engineering, Columbia University, 918 Mudd, New York, NY 10027.
E-mail: gg2138@columbia.edu

up through the troposphere and weaken the stratospheric polar vortex, which then causes upper-tropospheric stationary waves throughout the Northern Hemisphere to refract poleward. These hemispheric-scale coupled wave and mean flow anomalies then propagate down through the troposphere via a positive feedback, resulting in a downward-propagating negative AO anomaly during the winter season from the stratosphere to the surface. This teleconnection pathway will be referred to extensively throughout this paper.

These studies consistently point to Eurasia, and specifically Siberia, as the critical region for snow-forced winter AO anomalies. This is not altogether surprising, given that Siberia is a large, contiguous landmass characterized by extensive and variable snow conditions. Nonetheless, it is of interest to understand the specific physical and dynamical reasons why land surface snow anomalies in this region can influence winter climate on a hemispheric scale. One possible factor is the presence of large mountain ranges along the southern and eastern borders of Siberia. Cohen et al. (2001) describes an apparent poleward migration of observed autumn Siberian high pressure anomalies, which eventually form the winter AO pattern, and suggests that the expected eastward downgradient migration is impeded by these high orographic barriers. More importantly, the stationary wave activity, used as a diagnostic measure in Saito et al. (2001) and GEC03, originates in part from orographic obstructions (Plumb 1985; Ringler and Cook 1999). Recently, Kornich et al. (2003) reported the importance of both orography and land–sea heating contrasts for reproducing a downward-propagating stratospheric annular mode in an idealized winter GCM experiment. Other GCM studies highlight the sensitivity of planetary waves and stratospheric–tropospheric coupling to surface orographic amplitude (Taguchi et al. 2001; Taguchi and Yoden 2002; Walker and Magnusdottir 2003).

In this study, the role of orography in enabling a Siberian snow-forced winter AO response is investigated using GCM simulations analogous to those employed in GEC03. A pair of snow-forced ensemble experiments is performed in which the model's orographic boundary condition in central and eastern Siberia is limited to a maximum elevation of roughly 400 m. The ensemble mean climate response to the GEC03 positive Siberian snow perturbation is evaluated for these ''no-mountain'' experiments, and compared to the climate response with mountains as described in GEC03. Section 2 describes the altered orographic boundary that was developed and applied to the model, and the snow-forced experiments that were conducted. Section 3 evaluates the Siberian snow-forced climate response without mountains. Section 4 investigates the effect of removing Siberian mountains on the snow–AO teleconnection pathway and associated stationary wave activity. Conclusions are presented in section 5.

2. No-mountain experiments

The basic structure of the experiments is unchanged from GEC03. Once again the Max-Planck Institute for Meteorology ECHAM3 GCM (Roeckner et al. 1992) is used at T42 spectral truncation (roughly 2.8° grid cell resolution). Each experiment consists of 20 independent realizations of a 6-month (September–February) model integration period, in order to capture the interannual variability associated with the internal AO mode and to resolve externally forced climate impacts in the ensemble mean difference between two simulations. Ensemble member initial conditions are drawn from 1 September prognostics of a 20-yr control integration. As described in GEC03, one experiment prescribes grid cell snow water equivalent (SWE) over Siberia at each time step, derived from extensive snow conditions observed during September 1976–February 1977; the second experiment uses limited snow conditions observed during September 1988–February 1989 (Robinson et al. 1993). Ensemble mean differences between the two experiments are computed (extensive snow − limited snow) to evaluate the climatic response to a positive snow perturbation over Siberia. The ensemble distribution is used to test the statistical significance of the differences in experiment averages, via the *t* test.

In addition to comprising a large, contiguous region subject to seasonal snow cover, Siberia is bordered to the south and east by some of the tallest mountain ranges in the world. The Altay Shan Sayan, Yablonovyy, and Cherski Mountains all consistently exceed 1000 m in elevation, with a peak elevation of roughly 4500 m at Mt. Belukha. Together with the Tibetan Plateau, they form a continuous southwest–northeast ridge between Nepal and the Arctic Ocean, as illustrated in Fig. 1a using National Oceanic and Atmospheric Administration (NOAA) 5-min-gridded elevation data (NOAA 1988). These high orographic barriers are largely responsible for the major upward, eastward, and primarily equatorward transmission of stationary wave energy that originates over Siberia (Plumb 1985). This Siberian wave activity center is mechanically forced by the orographic obstructions, and is also thermally forced by related diabatic heating anomalies (Ringler and Cook 1999).

The teleconnection pathway relating Siberian snow anomalies to the winter AO mode, described in GEC03 and summarized in section 1, is initiated by additional forcing of the Siberia wave activity center. A positive Siberian snow perturbation produces a local negative diabatic heating anomaly, via various processes, including increased albedo, thermal emissivity and latent heat via snowmelt, and decreased thermal conductivity. The heating anomaly acts as an added surface thermal forcing on the orographically generated overlying stationary wave activity. An upward vertical wave activity flux anomaly is produced at the surface, and propagates through the troposphere and into the stratosphere.

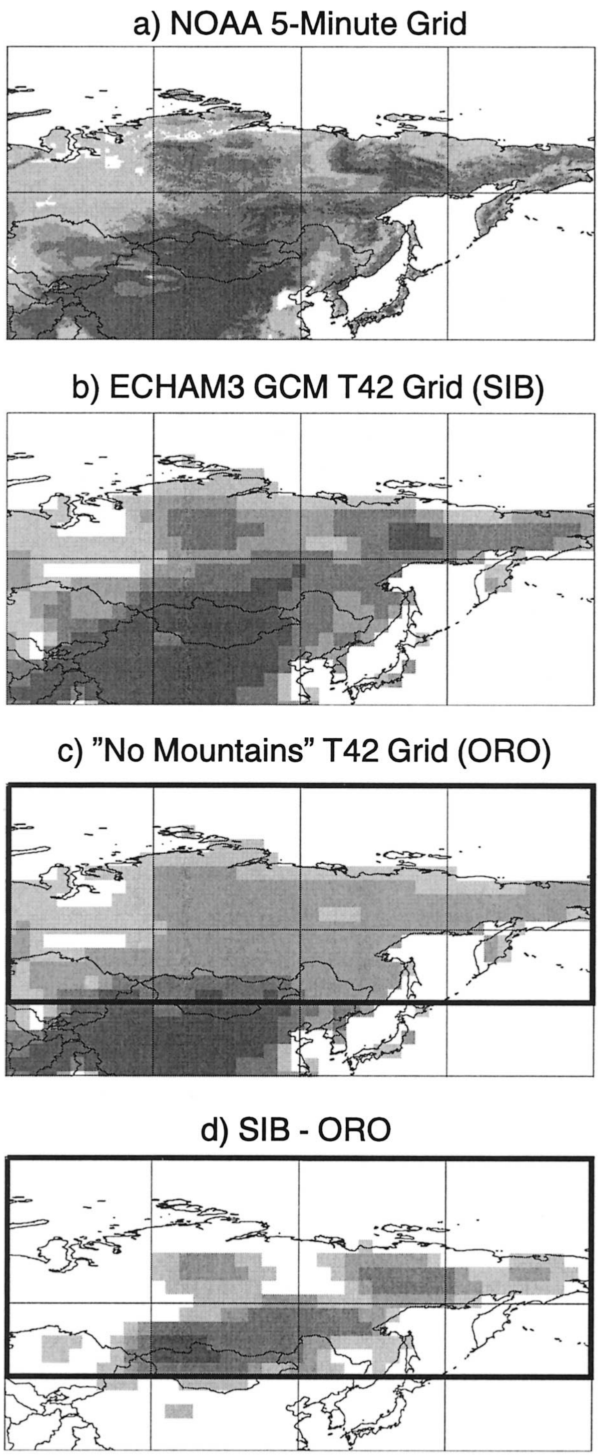

FIG. 1. Land surface orography over Siberia. Shading represents 50–200 (lightest), 200–400, 400–1000, and 1000+ (darkest) m. (a) NOAA 5-min-gridded data. (b) ECHAM3 GCM at T42 resolution (SIB). (c) Adjusted orography for no-mountain experiments (ORO). (d) Difference between SIB and ORO. Box indicates region in which model orography was adjusted.

Therefore, it is reasonable to expect that the snow–AO pathway is a direct consequence of the high orographic barriers that border Siberia to the south and east.

To investigate this hypothesis, a pair of GCM experiments is performed in which these barriers are reduced as a model boundary condition. But before conducting these no-mountain experiments, it is prudent to evaluate the orography that is applied in the base ECHAM3 model. The U.S. Navy 10-min global elevation dataset (Cuming and Hawkins 1981) was used to develop grid cell average surface elevations for the ECHAM3 model; T42 resolution elevations over Asia are shown in Fig. 1b. A comparison of Figs. 1a and 1b demonstrates that the orography over Asia is reasonably well represented by the model, and that the high-elevation mountains adjacent to Siberia are sufficiently resolved.

The orographically generated region of stationary wave activity originating in Siberia is similarly well represented by the model. Figure 2 shows the wintertime [December–January–February (DJF)] three-dimensional stationary wave activity flux (WAF) over the extratropical Northern Hemisphere, produced by a 20-yr control simulation of the base ECHAM3 model, for comparison, against observed fluxes presented in Fig. 4 of Plumb (1985). At 500 hPa (Fig. 2a), a large area of predominantly upward and eastward wave activity is centered over Siberia and far-east Asia, with an equatorward component at midlatitudes and a poleward component at high latitudes. A second major wave activity center over the North Atlantic is also simulated, as well as a small region of activity in western North America. Upper-level wave activity (150 hPa, Fig. 2b) also portrays the two major wave activity centers, propagating upward and equatorward. The modeled wave activity compares favorably to observations, although the modeled wave propagation is somewhat more equatorward and less eastward than observations. Overall, the ECHAM3 model serves as an appropriate platform for evaluating the role of orography in the Siberian snow–AO teleconnection pathway.

For the no-mountain experiments, an initial maximum elevation of 400 m is prescribed for all grid cells within 45°–90°N and 60°E–180° (see Fig. 1c). This region includes the mountains to the south and east of Siberia, but does not include the Tibetan plateau. The height and areal extent of the Tibetan plateau makes it influential to basic atmospheric dynamics, and its modification could result in large alterations to the general circulation of the modeled atmosphere. Grid cell elevations near the southern (45°N) border of the altered elevation region are adjusted to maintain a smooth gradient with the Tibetan plateau to the south. Other numerical adjustments were performed to ensure the stability and robustness of the model. The revised orography was spectrally fitted to the T42 resolution that was used, to filter out noise associated with spectral resolution inconsistencies. Also, the global mean surface pressure

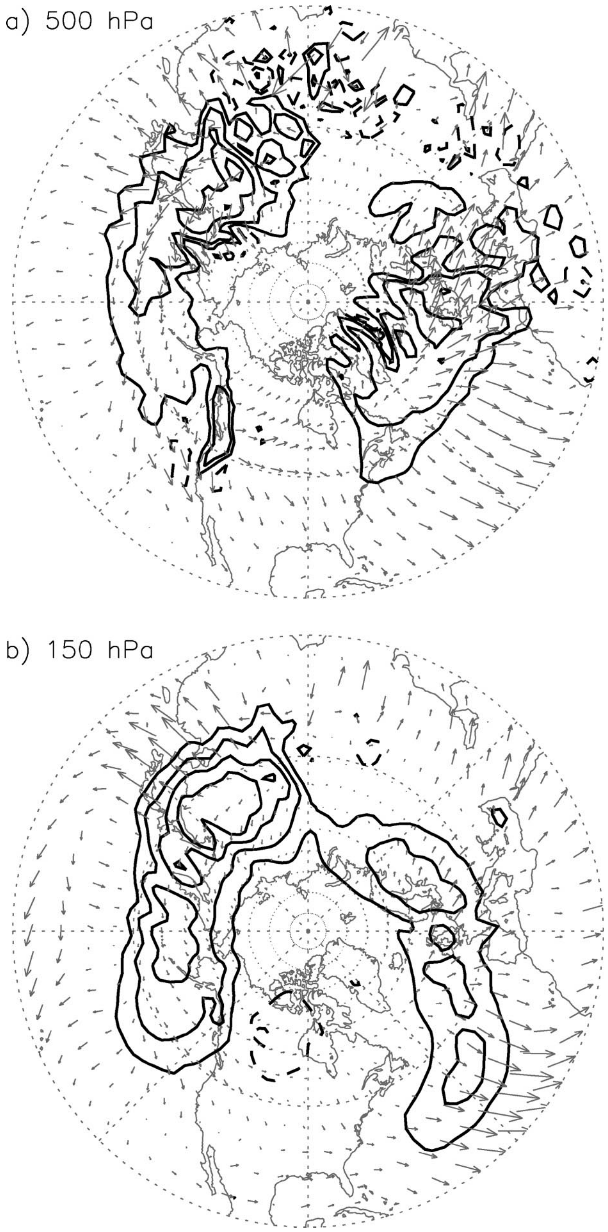

FIG. 2. Mean winter (DJF) three-dimensional wave activity flux climatology over the extratropical Northern Hemisphere, from a 20-yr control simulation of the ECHAM3 GCM. The pattern and magnitude of the wave activity flux compares well with those calculated by Plumb (1985), based on observations. Two centers are evident, one located over Siberia and another over the North Atlantic. Vectors denote horizontal fluxes (scale indicated on figure) and contours denote vertical fluxes. Dashed line denotes negative contour value. (a) 500-hPa elevation. Contour intervals drawn at ±0.03, 0.07, 0.15, 0.25 $m^2\ s^{-2}$. (b) 150-hPa elevation. Contour intervals drawn at ±0.01, 0.02, 0.03, 0.04 $m^2\ s^{-2}$.

(specified as a model boundary condition) was increased by 1.2 hPa to maintain a global mean sea level pressure of roughly 1013 hPa. This slight surface pressure boundary condition must increase to account for the additional air mass that results from lowering surface elevations, which generally has a negligible impact on the overall general circulation of the ECHAM3 model (U. Schlese 2002, personal communication).

The final Siberian surface elevations applied in the no-mountain experiments are shown in Fig. 1c. Aside from the southern border, elevations throughout the adjusted Siberian region are less than 400 m, with most of the region below 300 m. The 1000-m ridge that formerly extended northeast from Nepal to the Arctic Ocean now terminates in Mongolia. Figure 1d presents the difference between the base GCM orography and the no-mountain orography (i.e., Figs. 1b,c). The orography changes primarily consist of reduced elevations along the Siberian ridge, and also a slight lowering of the plateau located south of the Taimyr Peninsula. Due to the spectral fitting that was applied, nonmountainous regions in northern and western Siberia were slightly modified, though the magnitude of these elevation changes were generally within ±50 m. This adjusted orographic boundary condition is applied to both the extensive snow and limited snow GCM experiments performed for this study.

For this paper, the resulting ensemble mean response to snow without Siberian mountains will be denoted as ORO. The analogous ensemble mean response to snow with Siberian mountains, detailed in GEC03, will be denoted SIB. The negative winter AO-type response to snow and the associated teleconnection pathway that occurred for SIB will now be reevaluated for ORO. The similarities and/or differences between them will be studied to assess the extent to which the orographic barriers south and east of Siberia constrain the modeled snow–AO relationship.

3. AO mode modulation in response to snow without Siberian mountains

As described in GEC03, SIB generates a clear local surface climatic response in autumn to a positive snow perturbation over Siberia, in the form of higher albedo, lower temperature, and higher sea level pressure (SLP). The snow forcing and corresponding local thermodynamical response are both maintained during the winter, while responses beyond the Siberian forcing region are also produced, culminating in a hemispheric-scale SLP dynamical response that is indicative of a negative AO mode. The SIB seasonal mean surface temperature and SLP response is summarized in Fig. 3, which is repeated from GEC03's Figs. 4b,c,e,f. The negative winter AO response is clearly indicated in Fig. 3d by a large positive SLP anomaly over the arctic and broad negative SLP anomalies at midlatitudes, centered about the North Pacific and North Atlantic Oceans.

The corresponding fields for ORO are presented in Fig. 4. The local autumn surface thermodynamical response to snow is once again simulated, as indicated by lower temperatures in Fig. 4a and higher SLP in Fig. 4b. This is not surprising, because the snow forcing is identical

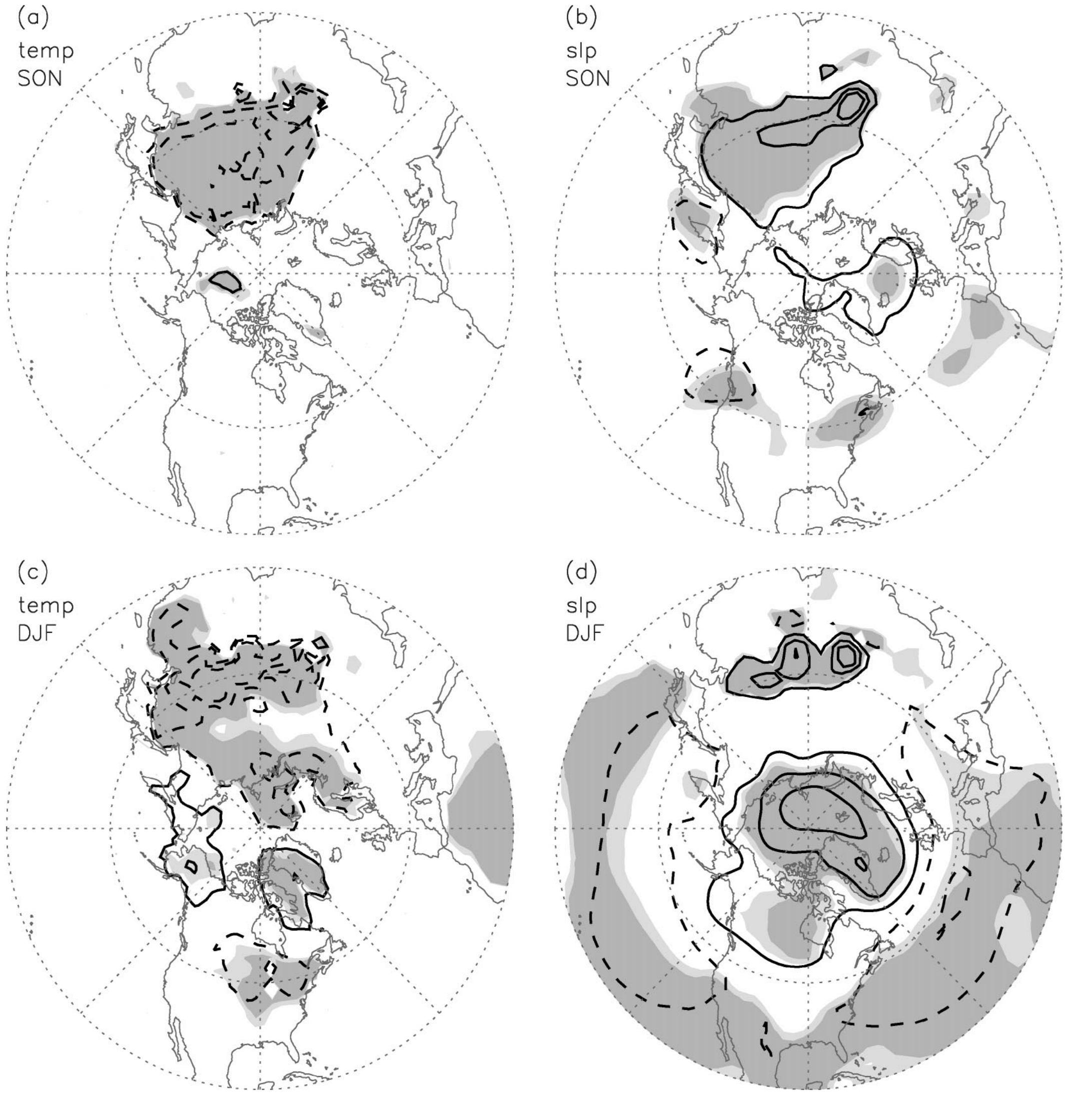

FIG. 3. Surface climatic response to positive Siberian snow forcing over the extratropical Northern Hemisphere for SIB, during (a), (b) autumn and (c), (d) winter seasons. (a), (c) Surface temperature contours drawn at ±1°, 3°, 5°C. (b), (d) Sea level pressure contours drawn at ±1, 3, 5 hPa. Dashed line denotes negative contour value. Light (dark) shading indicates 90% (95%) statistical significance.

for SIB and ORO. In winter, however (Figs. 4c,d), the surface temperature anomaly is much more localized, and the SLP anomaly field no longer produces a negative AO-type response. Rather than the fully formed positive (negative) SLP anomalies at high (mid-) latitudes seen for SIB, ORO produces isolated negative responses over the far North Atlantic and North Pacific, and produces similarly disconnected positive responses over western North America, central and eastern Asia, and the western North Atlantic. If anything, in the absence of Siberian mountains the winter SLP response to Siberian snow resembles a weakly positive AO mode.

In GEC03, an unstandardized AO index metric was developed to facilitate a quantitative comparison between the extensive and limited snow experiments. It is computed at the surface using the SLP field by subtracting the average value north of 61.5°N from the average value within the zonal band from 28° to 50°N; these two regions capture the centers of action in the ECHAM3 control SLP EOF-1 field, presented in Gong et al. (2002). This metric is used once again to evaluate the AO-type response to snow throughout the atmospheric column, as it evolves over the autumn–winter season. In Fig. 5 we present the weekly evolution of a 42-day moving average AO index response, computed using geopotential height differences between the two regions, and normalized over 12 atmospheric levels from 1000 to 10 hPa. SIB is shown in Fig. 5a (GEC03's Fig. 9), and ORO is shown in Fig. 5b. A major feature of the snow-forced negative AO signal is its character-

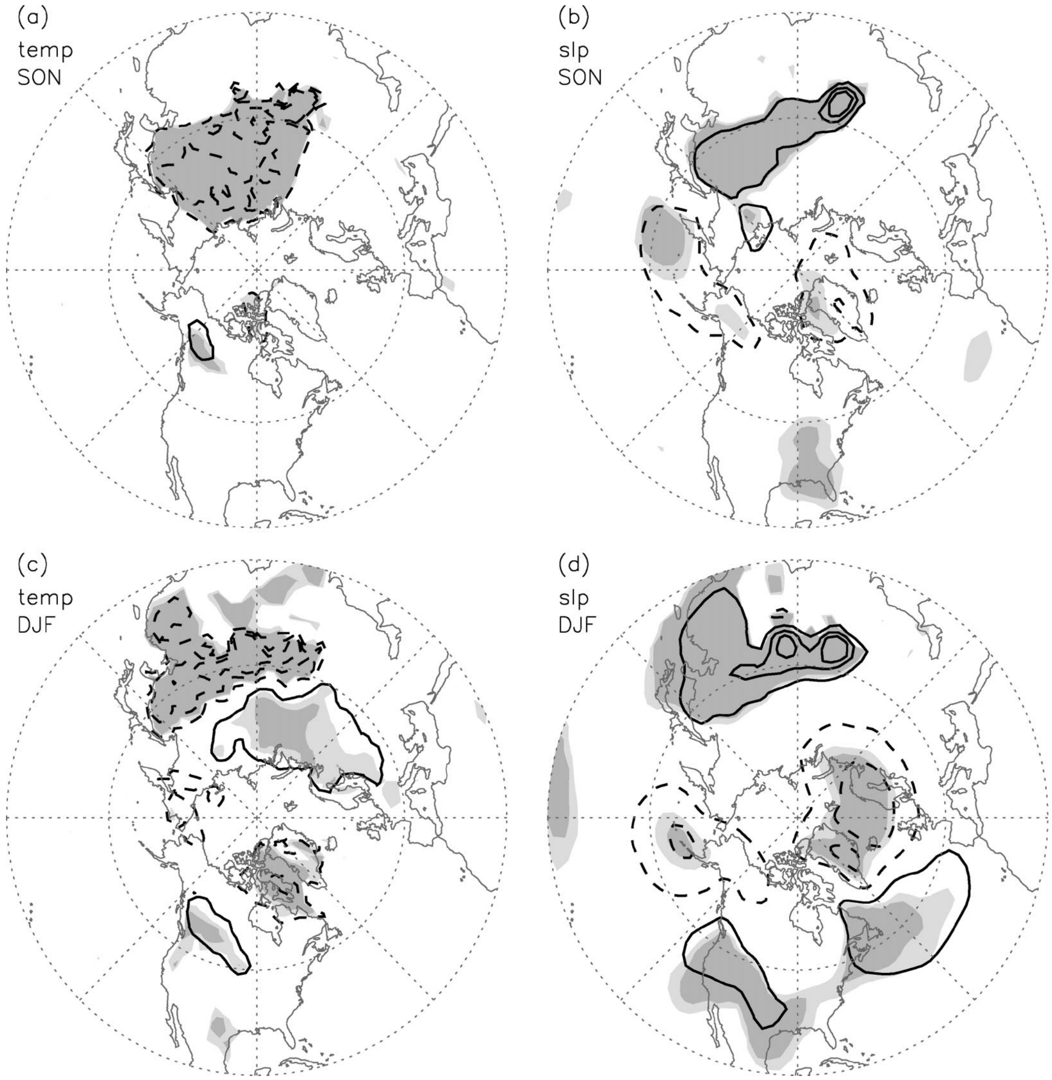

FIG. 4. Same as Fig. 3, but for ORO.

istic downward propagation from the stratosphere to the surface from late autumn through winter. This propagation pattern is clear in Fig. 5a, but is not evident in Fig. 5b. Furthermore, in Fig. 5a the initial late-autumn negative AO signal in the stratosphere indicates a decrease in geopotential height with latitude, and, thus, serves as an expression of the weakened polar vortex associated with the snow-forced AO mode modulation. In Fig. 5b this weakened vortex, from which the downward propagation originates, also fails to materialize. Thus, rather than just suppressing the ultimate surface negative winter AO response to Siberian snow, as indicated in Fig. 4d, the absence of Siberian mountains inhibits the entire snow-forced AO signal, throughout the atmospheric column, and over the entire autumn–winter season.

Instead of producing a downward-propagating negative AO signal, Fig. 5b indicates that ORO produces a significant positive AO signal during the late winter, extending throughout the troposphere and into the lower stratosphere. For the 3-month winter (DJF) seasonal mean, the normalized AO index at the surface, 500 hPa, and 50 hPa exhibit statistically significant (at least 94%) increases of 0.64, 0.60, and 0.62 standard deviations, respectively. These quantitative AO index results over the atmospheric column are consistent with the weakly positive snow-forced surface AO pattern produced for ORO in Fig. 4d. In contrast to Fig. 5a (SIB), no clear temporal propagation pathway is evident in Fig. 5b (ORO), which leads to the positive late-winter AO signal.

Clearly, the mountains to the south and east of Siberia are critical to the modeled negative winter AO mode modulation in response to a positive Siberian snow perturbation. When these orographic barriers are reduced as model boundary conditions in ORO, the downward-

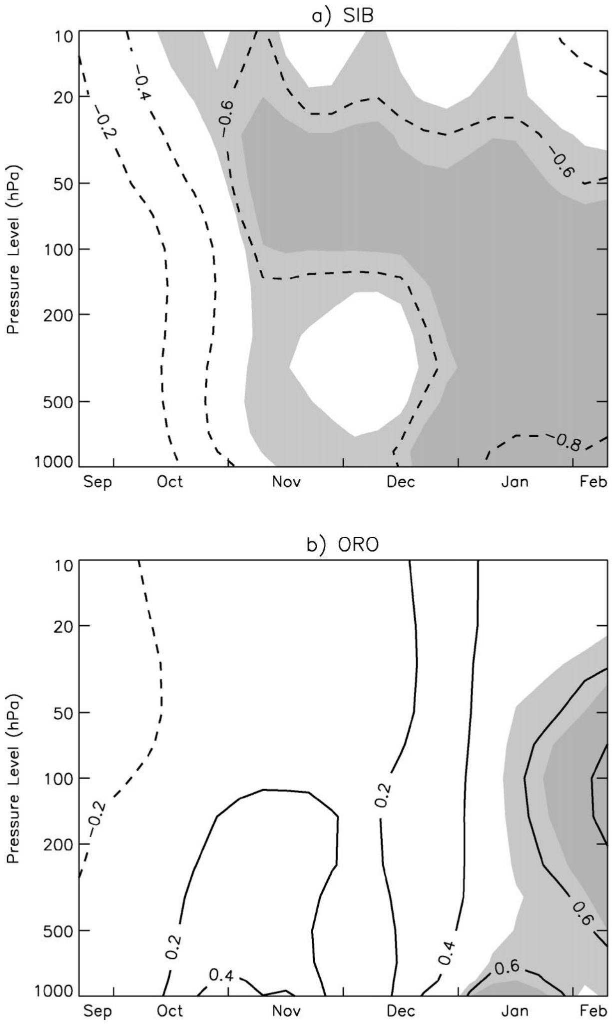

FIG. 5. Weekly evolution (horizontal axis) over the atmospheric column (vertical axis) of normalized 42-day moving average hemispheric AO index (difference between the average SLP north of 61.5°N and the average SLP within the zonal band from 28° to 50°N) response to positive Siberian snow forcing. Contours drawn at ±2, 4, 6, 8 standard deviations. Dashed line denotes negative contour value. Light (dark) shading indicates 90% (95%) statistical significance. (a) SIB and (b) ORO.

propagating AO signal from the stratosphere to the surface from late autumn through winter is no longer produced. This suggests that the vertical atmospheric teleconnection pathway described in GEC03, involving upward-propagating stationary wave anomalies followed by a weakened stratospheric polar vortex and downward-propagating wave and mean flow anomalies, breaks down at an early stage in the absence of Siberian mountains. Thus, these mountains represent an orographic constraint on the aforementioned snow–AO teleconnection pathway.

A question that naturally arises from this result is as follows: at what stage does the absence of Siberian mountains disrupt the snow–AO teleconnection pathway? This question will be addressed in the next section by analyzing stationary wave activity and its response to snow, for the ORO experiments. Furthermore, the apparent positive late-winter AO-type response to a positive Siberian snow perturbation for ORO is opposite to that of the expected and physically justified negative AO-type response for SIB. Therefore, a second question, which will be briefly considered, is as follows: can the apparent positive AO signal without Siberian mountains be explained via physical mechanisms? One hypothesis is put forth in the next section, within the context of the snow–AO teleconnection pathway.

4. Stationary wave activity without Siberian mountains

a. Disruption of the snow—AO teleconnection pathway

It was demonstrated in section 2 that the control ECHAM3 GCM does a credible job of reproducing the stationary wave activity throughout the Northern Hemisphere, including the orographically generated Siberian wave activity center. The effect of removing Siberian mountains on this prevailing stationary wave energy transmission will now be investigated. Figure 6 shows the seasonal average vertical WAF at 500 hPa over the extratropical Northern Hemisphere for SIB, averaged over all 40 realizations that comprise both the extensive and limited snow experiments. Two centers of stationary wave activity over eastern Siberia and the North Atlantic are clearly evident in winter (Fig. 6b). In autumn (Fig. 6a), these centers are already apparent, but have not yet fully developed, especially over the North Atlantic.

Figure 7 shows the corresponding vertical WAF field at 500 hPa for ORO. Under identical snow-forcing conditions, but in the absence of Siberian mountains, the two centers of stationary wave activity are still evident, but the magnitude of the upward activity over Siberia is notably reduced in both autumn and winter. Figure 8 shows the difference (SIB − ORO) for each season. At the heart of this wave activity center over far-east Asia, the vertical WAF decreases by as much as 50% in the absence of Siberian mountains, for both autumn and winter. The changes indicated in Fig. 8 throughout east Asia and the North Pacific are statistically significant at the 95% level. Stationary wave activity over Siberia is in all likelihood sustained in ORO by the dominant extratropical orographic barriers represented by the Tibetan plateau, but removing the mid- to high-latitude mountains in Siberia has a clear damping effect. Similarly, the eastward and equatorward components of the Siberia wave activity center (not shown) are substantially reduced but not altogether removed when Siberian mountains are removed. Note in Figs. 6–8 that the North Atlantic center is more or less unchanged between SIB and ORO, indicating that the impact on stationary wave activity is regional in scale, not global.

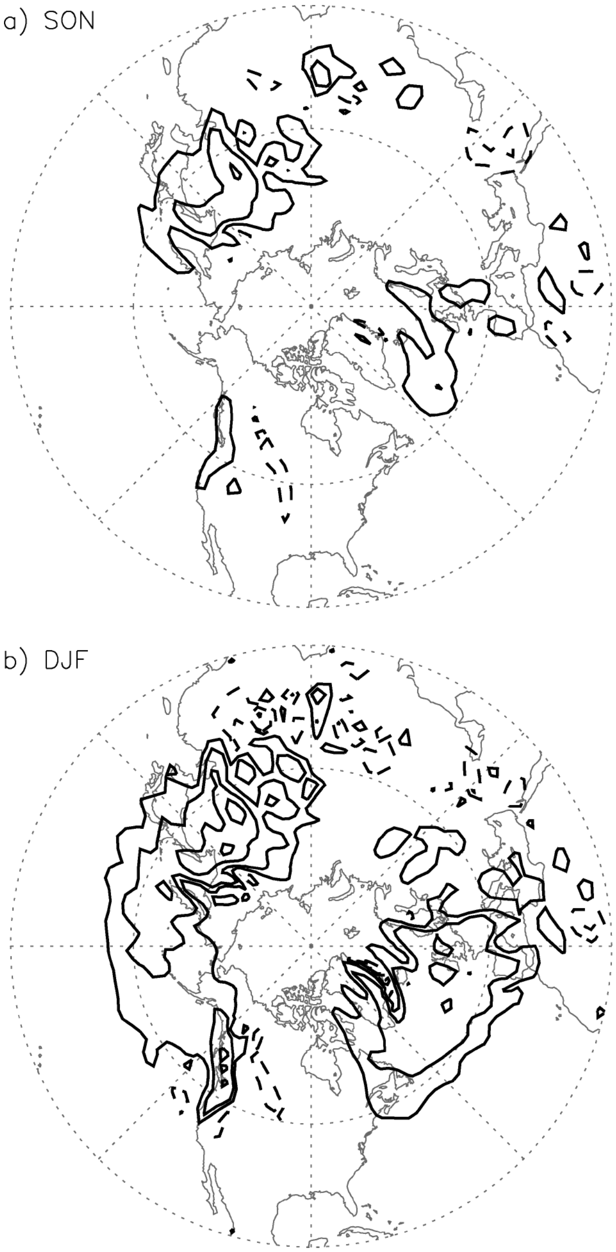

FIG. 6. Seasonal average vertical wave activity flux at 500-hPa elevation over the extratropical Northern Hemisphere for SIB, averaged over 40 ensemble realizations that comprise both extensive and limited snow experiments. Contour intervals drawn at ± 0.03, 0.07, 0.15, 0.25 $m^2 s^{-2}$. Dashed line denotes negative contour value.

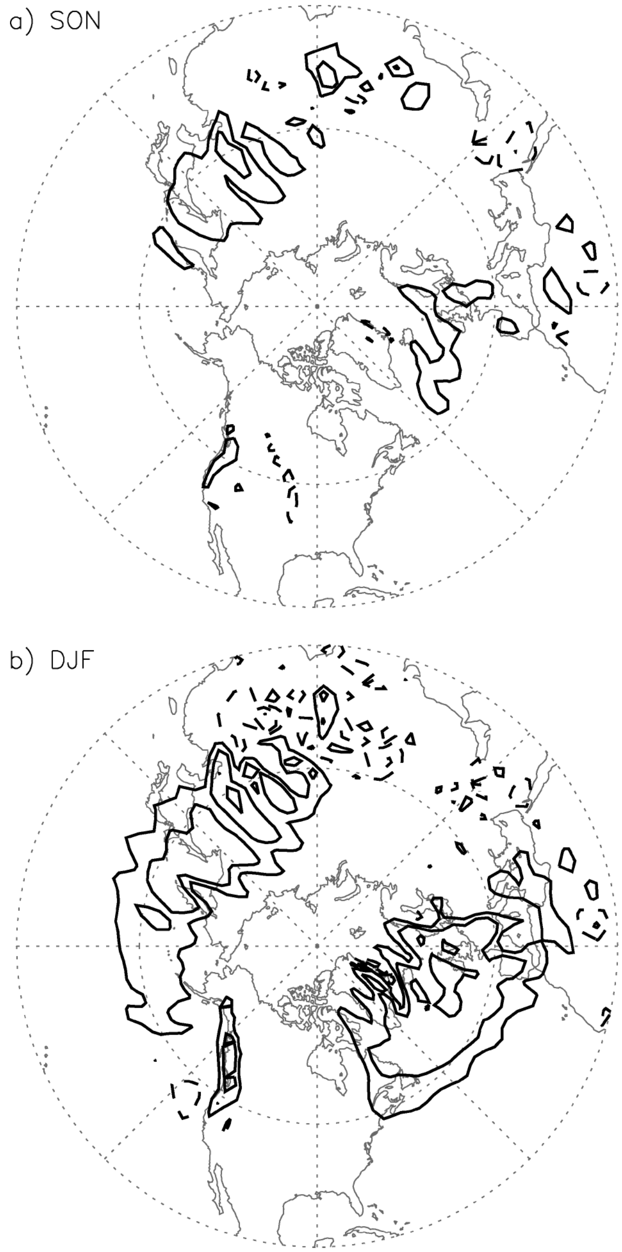

FIG. 7. Same as Fig. 6, except for ORO.

In the SIB experiments, the Siberian snow perturbations are collocated within a region of major stationary activity. Resulting diabatic heating anomalies, commonly associated with regional snow anomalies via various local thermodynamic processes (GEC03), generate an additional thermal forcing of this wave activity center. This produces a large local upward WAF anomaly over Siberia during autumn, as shown in Fig. 9a (GEC03's Fig. 5). For ORO, the same snow perturbation occurs within a substantially weakened stationary wave activity center. As a result, the autumn snow perturbation produces a more modest local upward WAF anomaly, in both magnitude and spatial extent, as shown in Fig. 9b.

For ORO, the combination of weaker vertical wave energy transmission and a diminished snow-forced upward WAF anomaly is insufficient to propel this thermally forced additional wave energy up through the troposphere and weaken the stratospheric polar vortex, as is the case for SIB as reported in observations (Kuroda and Kodera 1999; Limpasuvan and Hartmann

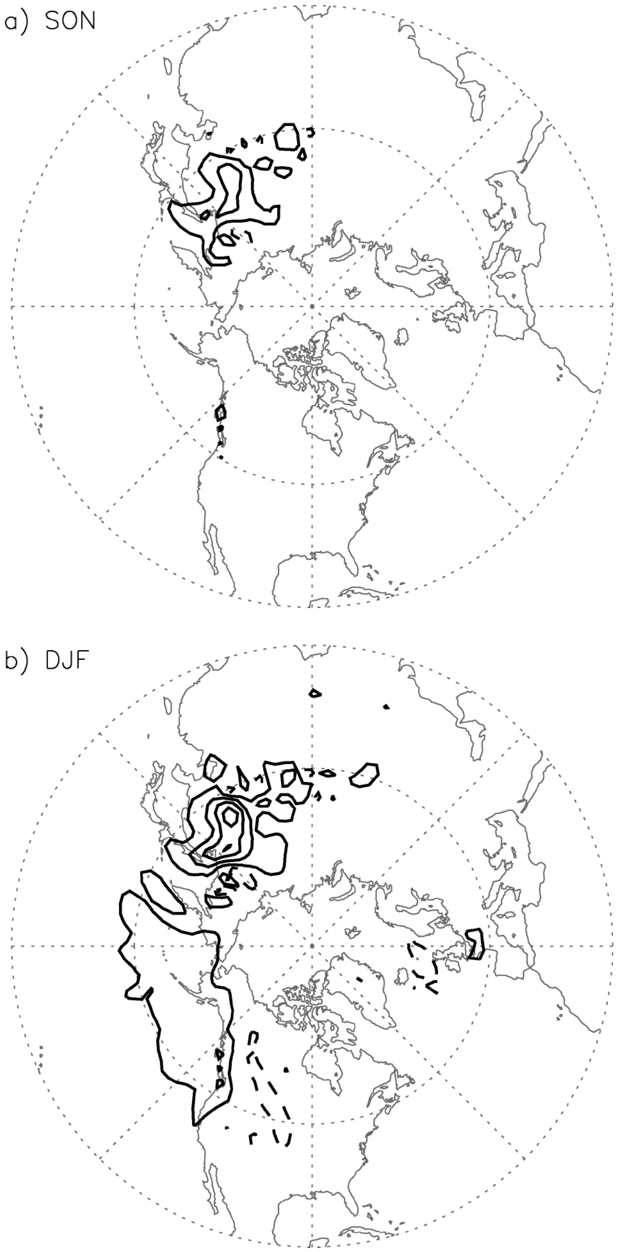

FIG. 8. Same as Fig. 6, except for the difference between SIB and ORO. Contour intervals drawn at ±0.02, 0.06, 0.10, 0.16 $m^2 s^{-2}$. Dashed line denotes negative contour value.

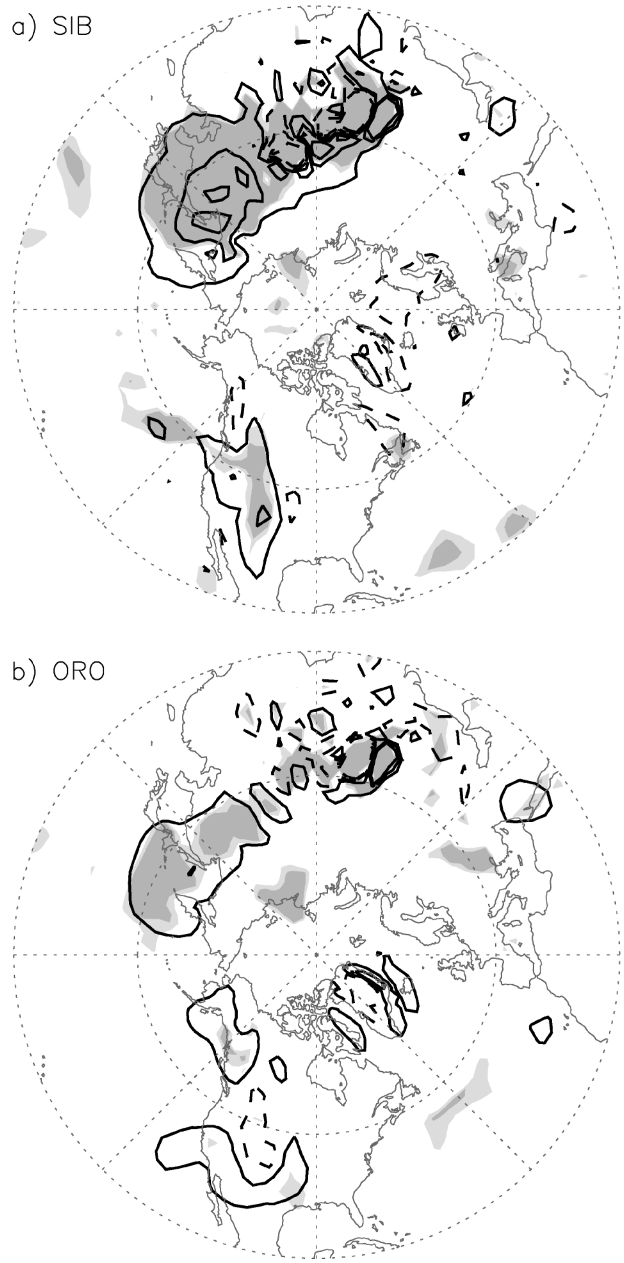

FIG. 9. Vertical wave activity flux response to positive Siberian snow forcing at 850-hPa elevation over the extratropical Northern Hemisphere, for autumn. Contours drawn at ±0.01, 0.04, 0.08 $m^2 s^{-2}$. Dashed line denotes negative contour value. Light (dark) shading indicates 90% (95%) statistical significance. (a) SIB and (b) ORO.

2000). Figures 10a and 10b show latitude versus pressure profiles of the WAF response over the Siberian wave activity center for SIB (GEC03's Figs. 6e and 7e). Figures 10c and 10d show analogous profiles for ORO. For a 42-day average period (Figs. 10a,c), a snow-forced upward WAF anomaly is evident near the surface over the Siberia wave activity center, but generally diminishes with elevation. The anomaly extends into the lower stratosphere for SIB, but not for ORO. For a particular weekly average period (Figs. 10b,d), the low-level upward WAF anomaly is notably larger, consistent with the notion expressed in GEC03 that these snow-forced anomalies are not continuous, but instead occur as a series of transient pulses throughout the autumn–winter season. For SIB, this upward anomaly pulse propagates up through the troposphere, and well into the stratosphere. For ORO the pulse also propagates up into the troposphere, but fails to break through to the stratosphere.

Figure 10 exemplifies typical WAF transient-pulse

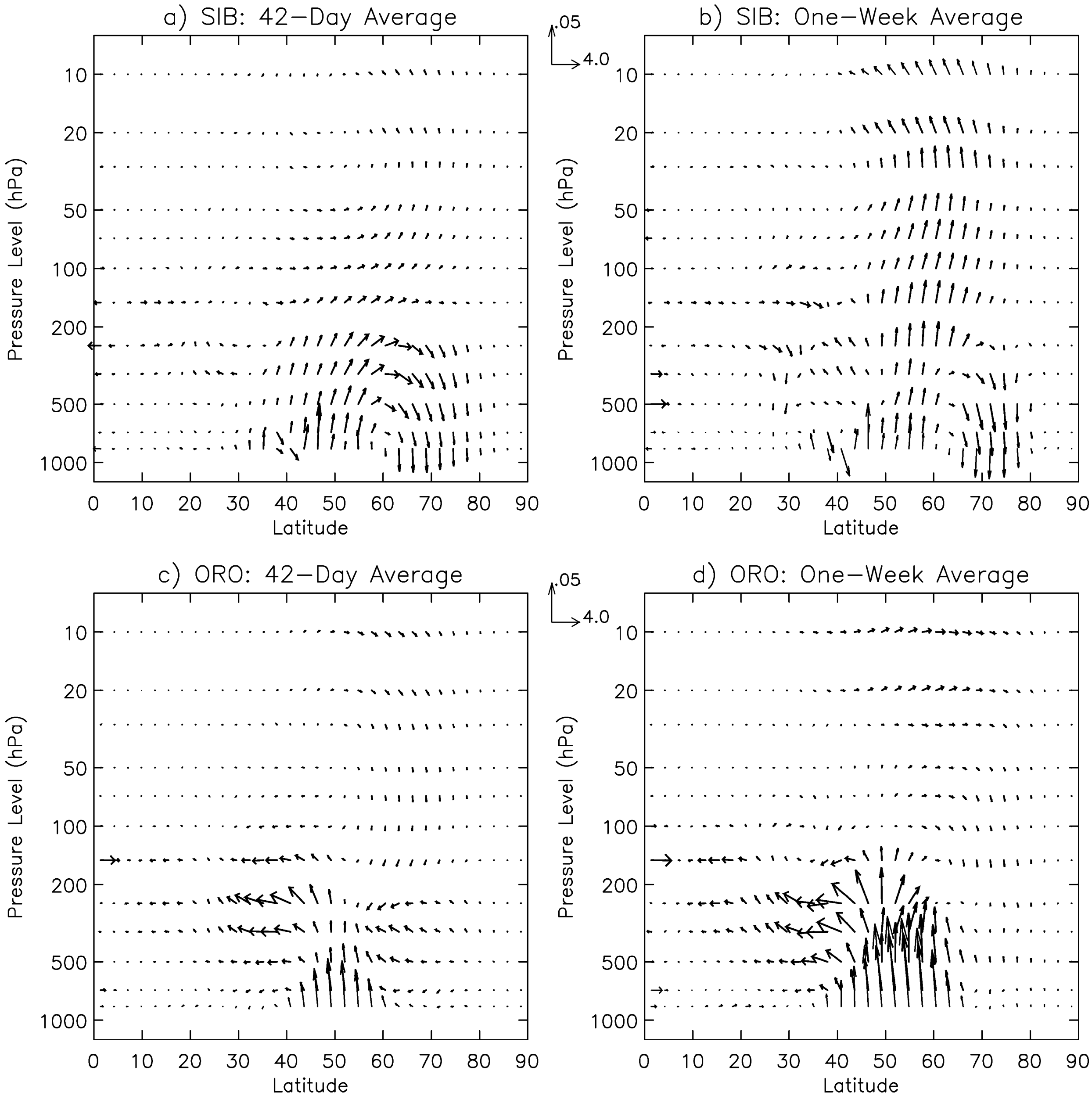

FIG. 10. Latitude (0°–90°N) vs pressure level (850–10 hPa) profiles of wave activity flux response to positive Siberian snow forcing. Vectors represent meridional and vertical fluxes averaged over the Siberia wave activity center (scale in $m^2 s^{-2}$ is indicated on figure). (a) The 42-day average period in mid-December, for SIB. (b) The 1-week average period in mid-Dec, for SIB. (c) The 42-day average period in mid-Nov, for ORO. (d) The 1-week average period in mid-Nov, for ORO.

response profiles during the course of the autumn–winter simulation period. Thus, without Siberian mountains, the initial component of the snow–AO teleconnection pathway (i.e., upward propagation of tropospheric wave anomalies) does occur, but is weakened considerably. The anomaly fails to extend into the stratosphere and weaken the polar vortex, thereby disrupting the teleconnection. Because the local upward WAF response to the Siberian snow perturbation (Fig. 9) is dependent on the orographic barriers adjacent to Siberia, removal of these barriers suppresses this local response and prevents the subsequent remote teleconnection response from fully developing.

Note that the weekly average metric in Figs. 10b and 10d effectively portrays the magnitude of each transient pulse, while the 42-day average metric in Figs. 10a and 10c provide a smoothed response signal derived from the series of transient pulses, in excess of short-term fluctuations. In other words, the 42-day average filters out the ‘‘climate noise’’ without averaging out the pulselike signal. This metric is, thus, well-suited for evaluating the temporal evolution of the overall climatic response, shown in Fig. 5. Possible reasons for the transient pulselike nature of the WAF response include spatial and/or temporal variations in the observation-based snow forcing, and temporal variations in the ambient WAF field (please refer to GEC03 for details).

b. *Hypothesized interpretation for the apparent positive AO mode modulation*

We end by briefly hypothesizing one possible interpretation for the apparent positive AO-type response that occurs for ORO, within the context of stationary wave activity and the snow–AO teleconnection pathway. Although the snow-forced upward WAF anomaly is notably diminished for ORO, some additional thermally forced wave energy is nevertheless introduced into the atmosphere by the Siberian snow perturbation. Instead of the downward-propagating poleward wave refraction seen for SIB, the primary horizontal stationary wave response for ORO appears to be a hemispheric-scale equatorward refraction throughout the troposphere. The poleward (equatorward) refraction for SIB (ORO) is evident over the Siberian wave activity center in Figs. 10a and 10b (Figs. 10c and 10d). In both sets of experiments, the meridional wave refraction is restricted to the troposphere. Furthermore, Fig. 11 shows snow-forced horizontal WAF anomaly vectors in the upper troposphere (250 hPa), during winter (DJF), for SIB (GEC03's Fig. 8) and ORO. The hemispheric-scale of the poleward (equatorward) refraction for SIB (ORO) is evident over the midlatitudes, concentrated near the two dominant centers of wave activity over Siberia and the North Atlantic.

Note that for both sets of experiments, the local snow-forced upward WAF anomaly over Siberia (Fig. 9) evolves into a hemispheric-scale meridional WAF anomaly (Fig. 11). For SIB this anomaly development occurs via interaction with the stratospheric polar vortex (GEC03), but for ORO the pathway is unclear. One possible interpretation is that the additional thermally forced wave energy excites the prevailing equatorward component of the planetary Rossby waves. Without Siberian mountains, the snow-forced upward WAF anomaly does not propagate up through the entire troposphere to weaken the stratospheric polar vortex. This anomalous energy, therefore, remains in the troposphere, where it simply acts to enhance the dominant tropospheric wave activity centers over Siberia and the North Atlantic. Because the prevailing wave energy spreads upward and equatorward, the added wave energy is manifested as an equatorward anomaly that spreads throughout the troposphere. The eastward component of the wave energy transmission allows the added energy to be distributed throughout the Northern Hemisphere, although eastward anomalies are negligible compared to equatorward ones in Fig. 11b. These hemispheric-scale equatorward WAF anomalies are indicative of poleward momentum flux anomalies (Zhou et al. 2001), which produce dipole mean flow anomalies consistent with the positive AO mode modulation shown in Fig. 5b. For ORO, this is exemplified by positive (negative) zonal mean zonal wind anomalies at higher (lower) latitudes (not shown).

Hence, the positive AO-type response that occurs for ORO may result from a simple enhancement of the prevailing equatorward stationary wave activity. The ul-

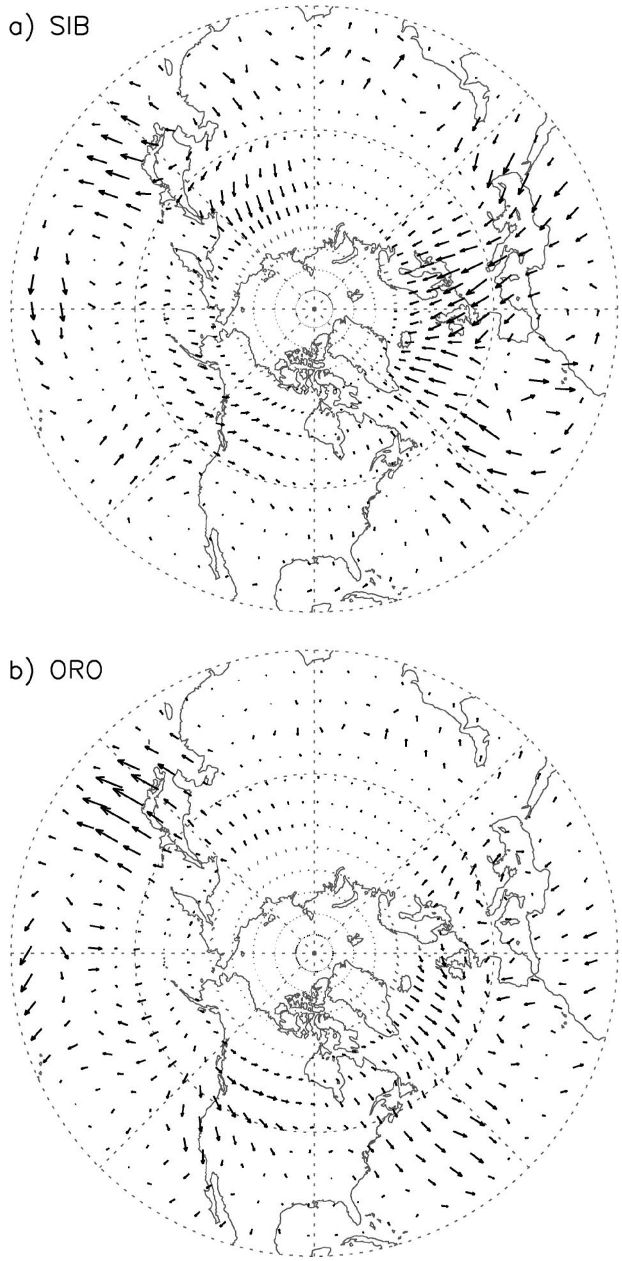

FIG. 11. Horizontal wave activity flux response to positive Siberian snow forcing, at 250-hPa elevation over the extratropical Northern Hemisphere, for winter (DJF). Largest vector drawn represents 12 $m^2 s^{-2}$. (a) SIB and (b) ORO.

timate positive AO anomaly occurs considerably later than the negative AO-type response in SIB (Fig. 5), for two likely reasons. First, the initial upward WAF anomaly is weaker for ORO (Fig. 9), so that there is less energy input to perturb the atmospheric circulation. Second, a positive feedback mechanism was identified for SIB in GEC03 between downward-propagating mean flow anomalies and poleward wave refraction, such that there was a perpetual forcing of the poleward WAF anomalies. For ORO, no such feedback mechanism is apparent, and the equatorward WAF anomalies are more modest (Fig. 11). Thus, the equatorward wave refraction is driven only by relatively mild snow-forced pulses of added wave energy, which gradually accumulate over the autumn–winter season, and eventually yield a positive AO-type response in late winter.

This hypothesized interpretation for the positive AO-type response for ORO is not as clear as the vertical teleconnection pathway and negative AO mode modulation identified for SIB. For example, why does the added wave energy enhance the meridional component of the prevailing wave activity, but not the zonal component? Also, how does the regional wave energy input over Siberia translate so rapidly into a hemispheric-scale equatorward refraction, without the aid of the stratosphere, as seen for SIB? A detailed analysis of the Rossby wave dynamics simulated by the model is required to answer these questions, which is outside the scope of the current study. Due to the limited extent of the positive AO index response shown in Fig. 5b, and the lack of a clear AO-type response in mean flow parameters such, as SLP in Fig. 4d, it is quite possible that this apparent positive AO response for ORO is simply due to random interannual fluctuations in the internal AO mode. Another possibility is that snow-forced hemispheric equatorward wave anomalies are artificially exaggerated by the ECHAM3 model, due to the fact that the equatorward component of the modeled wave activity is overpredicted compared to observations, as is acknowledged in section 2. In fact, it is not certain that the AO mode is affected at all in the ORO experiments, based on the ambiguity of the climatic response patterns in Fig. 4. Additional research is required to substantiate the preliminary interpretation hypothesized here.

5. Conclusions

Siberia has previously been identified as a critical region for producing snow-forced winter AO anomalies. In addition to being a large, contiguous land surface area subject to substantial seasonal snow cover variations, Siberia is bordered to the south and east by mountain ranges that consistently exceed 1000 m in elevation. The high orographic barriers in this region are mainly responsible for the large region of stationary wave energy transmission that originates over Siberia. Earlier studies have identified a clear atmospheric teleconnection pathway linking interannual early season snow variations over Siberia to interannual modulations of the winter AO mode (GEC03). A primary component of this teleconnection is the enhanced upward propagation of energy within this Siberian wave activity center, driven by snow-forced diabatic heating anomalies at the surface.

In this study, the role of the orographic barriers adjacent to Siberia in producing this snow–AO teleconnection pathway is investigated. The ECHAM3 GCM's orographic boundary condition is modified such that the downstream Siberian mountains are reduced. The ensemble mean response to a realistic Siberian snow forcing is then evaluated, in a manner consistent with previous studies. Model results indicate that without the Siberian mountains, the negative winter AO response to a positive Siberian snow forcing is no longer produced. Furthermore, the snow–AO teleconnection pathway fails to develop beyond the initial upward propagation of local snow-forced stationary wave energy into the troposphere. The propagation of stationary wave energy into the stratosphere, the subsequent weakening of the polar vortex, and the ultimate downward stratosphere-to-surface propagation of coupled wave–mean flow anomalies and associated AO signals, do not occur in the absence of Siberian mountains.

Thus, we conclude that the Siberian snow–winter AO relationship arises due to the specific and unique orographic conditions in the Siberian region. The mountains to the south and east of Siberia contribute substantially to the major center of stationary wave activity that is dominant over Siberia, especially in its upward-propagating component. The modeled snow perturbations are regionally collocated within this strong Siberian wave activity center, so that the associated thermal wave forcing is constrained to a large upward wave activity flux anomaly that extends through the tropopause, thereby resulting in the snow–AO teleconnection pathway. Therefore, the mountains adjacent to Siberia represent an orographic constraint on this modeled teleconnection pathway.

Without Siberian mountains, both the prevailing Siberian wave activity center and the snow-forced upward wave anomaly are considerably weaker, and the added wave energy is not forced to propagate all the way up to the stratosphere. Instead, this modest wave energy input remains in the troposphere, where it appears to enhance the prevailing centers of stationary wave activity over Siberia and the North Atlantic. We hypothesize that this produces a hemispheric-scale equatorward wave flux anomaly, and corresponding poleward momentum flux and dipole mean flow anomalies, which eventually yield the unexpected result of a positive AO-type response in late winter. The physical mechanisms behind this apparent snow-forced positive winter AO anomaly in the absence of Siberian mountains are still unclear. The ambiguous positive AO response may in fact be physically unrelated to the snow forcing, and simply arise from either random fluctuations in the fundamental, internal AO mode of atmospheric variability, or biases in the ECHAM3 GCM.

What is clear, however, is that the orographic conditions around Siberia are key to instigating the previously established positive Siberian snow–negative winter AO teleconnection pathway, which is physically justifiable (GEC03) and supported by other observational and modeling studies found in the literature (Baldwin and Dunkerton 1999; Kuroda and Kodera 1999; Limpasuvan and Hartmann 2000; Zhou et al. 2002). The results of the current study imply that snow anomalies over Siberia are capable of modulating the winter AO mode, due to its unique orographic features. Thus, a physical argument is provided here to support previous studies that identify Eurasia and Siberia as the critical region for snow-forced winter AO anomalies. Concurrent modeling studies have been conducted to further confirm this assertion, in which regions other than exclusively Siberia are forced with realistic snow perturbations (Gong et al. 2003b). Ongoing research investigates the linearity of the model response to snow forcings of different phase and magnitude, using long-term snow-forced simulation experiments. Issues of linearity cannot be adequately addressed using the experimental design employed here, because only the two limits of observed Siberian snow variability are simulated. The identification and full characterization of specific, influential snow-forcing regions for winter AO mode modulation will be advantageous to the prospective incorporation of land surface snow anomalies into future climate prediction efforts.

Acknowledgments. This investigation was supported by the National Science Foundation Grants ATM-9902433 and ATM-0127667. We would like to thank two anonymous reviewers for their insightful comments, and Drs. Ulruch Schlese and Joerg Wegner for their assistance with the ECHAM3 orography modifications.

REFERENCES

Baldwin, M. P., 2001: Annular modes in global daily surface pressure. *Geophys. Res. Lett.,* **28,** 4115–4118.

——, and T. J. Dunkerton, 1999: Propagation of the Arctic Oscillation from the stratosphere to the troposphere. *J. Geophys. Res.,* **104** (D24), 30 937–30 946.

Christiansen, B., 2000: A model study of the dynamical connection between the Arctic Oscillation and stratospheric vacillations. *J. Geophys. Res.,* **105** (D24), 29 461–29 474.

Cohen, J., 1994: Snow cover and climate. *Weather,* **49,** 150–156.

——, and D. Entekhabi, 1999: Eurasian snow cover variability and Northern Hemisphere climate predictability. *Geophys. Res. Lett.,* **26,** 345–348.

——, and ——, 2001: The influence of snow cover on Northern Hemisphere climate variability. *Atmos.–Ocean,* **39,** 35–53.

——, K. Saito, and D. Entekhabi, 2001: The role of the Siberian High in Northern Hemisphere climate variability. *Geophys. Res. Lett.,* **28,** 299–302.

Cuming, M. J., and B. A. Hawkins, 1981: TERDAT: The FNOC system for terrain data extraction and processing. Meteorology International Inc. Tech. Rep. MII Project M-254, 2d ed., prepared for USN/FNOC.

Feldstein, S. B., 2002: The recent trend and variance increase of the annular mode. *J. Climate,* **15,** 88–94.

Gong, G., D. Entekhabi, and J. Cohen, 2002: A large-ensemble model study of the wintertime AO/NAO and the role of interannual snow perturbations. *J. Climate,* **15,** 3488–3499.

——, ——, and ——, 2003a: Modeled Northern Hemisphere winter climate response to realistic Siberian snow anomalies. *J. Climate,* **16,** 3917–3931.

——, ——, and ——, 2003b: Relative Impacts of Siberian and North American snow anomalies on the winter Arctic Oscillation. *Geophys. Res. Lett.,* **30,** 1848, doi:10.1029/2003GLO17749.

Hurrell, J. W., 1995: Decadal trends in the North Atlantic Oscillation, regional temperatures and precipitation. *Science,* **269,** 676–679.

Kornich, H., G. Schmitz, and E. Becker, 2003: Dependence of the annular mode in the troposphere and stratosphere on orography and land–sea heating contrasts. *Geophys. Res. Lett.,* **30,** 1265, doi:10.129/2002GL016327.

Kuroda, Y., and K. Kodera, 1999: Role of planetary waves in stratosphere–troposphere coupled variability in the Northern Hemisphere winter. *Geophys. Res. Lett.,* **26,** 2375–2378.

Limpasuvan, V., and D. L. Hartmann, 2000: Wave-maintained annular modes of climate variability. *J. Climate,* **13,** 4414–4429.

NOAA, 1988: Digital relief of the Surface of the Earth. NOAA Data Announcement 88-MGG-02, National Geophysical Data Center.

Plumb, R. A., 1985: On the three-dimensional propagation of stationary waves. *J. Atmos. Sci.,* **42,** 217–229.

Ringler, T. D., and K. H. Cook, 1999: Understanding the seasonality of orographically forced waves: Interaction between mechanical and thermal forcing. *J. Atmos. Sci.,* **56,** 1154–1174.

Robertson, A. W., 2001: Influence of ocean–atmosphere interaction on the Arctic Oscillation in two general circulation models. *J. Climate,* **14,** 3240–3254.

Robinson, D. A., K. F. Dewey, and R. R. Heim Jr., 1993: Global snow cover monitoring: An update. *Bull. Amer. Meteor. Soc.,* **74,** 1689–1696.

Rodwell, M. J., D. P. Rowell, and C. K. Folland, 1999: Oceanic forcing of the wintertime North Atlantic Oscillation and European climate. *Nature,* **398,** 320–323.

Roeckner, E., and Coauthors, 1992: Simulation of the present-day climate with the ECHAM model: Impact of model physics and resolution. Max-Planck-Institute for Meteorology Rep. 93, 171 pp.

Saito, K., J. Cohen, and D. Entekhabi, 2001: Evolution of atmospheric response to early-season Eurasian snow cover anomalies. *Mon. Wea. Rev.,* **129,** 2746–2760.

Taguchi, M., and S. Yoden, 2002: Internal interannual variability of the troposphere–stratosphere coupled system in a simple global circulation model. Part I: Parameter sweep experiment. *J. Atmos. Sci.,* **59,** 3021–3036.

——, T. Yamaga, and S. Yoden, 2001: Internal variability of the troposphere–stratosphere coupled system simulated in a simple global circulation model. *J. Atmos. Sci.,* **58,** 3184–3203.

Thompson, D. W. J., and J. M. Wallace, 1998: The Arctic Oscillation signature in wintertime geopotential height and temperature fields. *Geophys. Res. Lett.,* **25,** 1297–1300.

——, and ——, 2001: Regional climate impacts of the Northern Hemisphere Annular Mode. *Science,* **293,** 85–89.

Walker, C. C., and G. Magnusdottir, 2003: Nonlinear planetary wave reflection in an atmospheric GCM. *J. Atmos. Sci.,* **60,** 279–286.

Walland, D. J., and I. Simmonds, 1997: Modelled atmospheric response to changes in Northern Hemisphere snow cover. *Climate Dyn.,* **13,** 25–34.

Watanabe, M., and T. Nitta, 1998: Relative impacts of snow and sea surface temperature anomalies on an extreme phase in the winter atmospheric circulation. *J. Climate,* **11,** 2837–2857.

——, and ——, 1999: Decadal changes in the atmospheric circulation and associated surface climate variations in the Northern Hemisphere winter. *J. Climate,* **12,** 494–509.

Zhou, S., A. J. Miller, J. Wang, and J. K. Angell, 2001: Trends of NAO and AO and their associations with stratospheric processes. *Geophys. Res. Lett.,* **28,** 4107–4110.

——, ——, ——, and ——, 2002: Downward-propagating temperature anomalies in the preconditioned polar stratosphere. *J. Climate,* **15,** 781–792.